NASA TN D-1733

38 p.

TECHNICAL NOTE

D-1733

NEUTRALIZER TESTS ON A FLIGHT-MODEL ELECTRON-BOMBARDMENT ION THRUSTOR

By Robert F. Kemp and J. M. Sellen, Jr.

Space Technology Laboratories, Inc.
Redondo Beach, California

and

Eugene V. Pawlik

Lewis Research Center
Cleveland, Ohio

NATIONAL AERONAUTICS AND SPACE ADMINISTRATION
WASHINGTON

July 1963

NATIONAL AERONAUTICS AND SPACE ADMINISTRATION

TECHNICAL NOTE D-1733

NEUTRALIZER TESTS ON A FLIGHT-MODEL ELECTRON-BOMBARDMENT ION THRUSTOR

By Robert F. Kemp, J. M. Sellen, Jr., and Eugene V. Pawlik[1]

SUMMARY

A series of neutralizer tests on a flight-test-design electron-bombardment ion thrustor is described that uses a pulsed-beam technique and utilizes a floating beam collector. The thrustor was operated at approximately flight-test design-point power levels. Electric potentials were measured with an electron emissive probe within the plasma exhaust beam for several neutralizer configurations. Measurements were also made of beam current density and neutralizer lifetimes.

With a net acceleration voltage of 2500 volts, a net- to total-voltage ratio of 0.56, and a beam current of 200 to 280 milliamperes, the plasma potential was 8 to 9 volts above that of the neutralizer for the original neutralizer configuration and ranged from this value to 0.9 volt for a number of other configurations. No increase in beam divergence due to inadequate neutralization was detected. Neutralizer lifetimes of 2 to 3 hours were typical and are adequate for a ballistic flight test. Shielded neutralizer configurations showed projected lifetimes greater than 50 hours.

INTRODUCTION

When the project reported herein was undertaken, the first NASA flight tests of electrostatic propulsion thrustors were in preparation. Some of the early doubts concerning whether or not space charge and current neutralization of ion propulsion beams could be made to occur in space had been allayed, and certain attempts had been made to operate ion thrustors in a simulated space environment (ref. 1). Central in these experiments was isolation of the thrustor from the physical boundaries of the vacuum enclosure, so that the thrustor neutralizer system was required to supply the beam with a current of electrons equal to the accelerated ion current. This was accomplished by two means: the pulsed-beam technique and the use of a floating collector. In the first technique, the

---

[1]The research reported herein was performed by Mr. Robert F. Kemp and Dr. J. M. Sellen, Jr., of Space Technology Laboratories of Redondo Beach, Calif. under contract with the National Aeronautics and Space Administration. Mr. Eugene V. Pawlik of the NASA Lewis Research Center was consultant for the project and assisted in the preparation of the report.

acceleration voltages were switched on rapidly. During the next several tens of microseconds, while the beam front traversed the length of the enclosure, measurements were made of the effectiveness of the neutralization process. In the second technique, the ion beam collector was electrically isolated from the common "ground", so that after the arrival of the beam at the collector, it assumed that particular potential at which equal currents of ions and electrons were collected. The difference between the floating-collector potential and that of the neutralizer was an approximate measure of the neutralization effectiveness. The ultimate measure of neutralization, during either the transient or steady-state period, was the potential of the plasma with respect to that of the neutralizer, as determined by a hot-wire probe capable of emitting a small electron current. This potential difference should be low to reduce random electron velocities and to permit more efficient thrustor operation.

It was the purpose of the present project to make such tests (ref. 2) on a flight-type electron-bombardment thrustor suitable for use on short duration flight tests to ensure the adequacy of the neutralizer system design. Other objectives were to establish the operating point for the neutralizer and to accumulate information that could be correlated with the results of the space test.

APPARATUS

The ion thrustor tested was a 10-centimeter-diameter beam flight-type supplied to Space Technology Laboratories by NASA Lewis Research Center. The general configuration and principles of operation are similar to those of the thrustors described in references 3 to 5. Figure 1 is a cutaway view of the thrustor that shows the structure in detail. Figure 2 shows the thrustor mounted on a proposed flight-test package. Figure 3 shows a flight-model thrustor mounted on the base plate that fits onto the vacuum facility. The principal differences between this thrustor and those on which data had previously been published are (1) the modified structure to accommodate the anticipated vibration levels during launch and (2) the use of electric heat for the boiler instead of steam. The flight-model boiler is fitted with a porous stainless-steel plug that allows mercury vapor to pass to the discharge chamber but retains the liquid because of the surface tension of mercury. For the pore size selected, the pressure drop between the boiler and the plasma chamber is much larger than previously noted. The boiler temperature is higher, and since it is no longer related to the steam point, it is more difficult to stabilize. The propellant system is more fully described in reference 6.

Thrustor Power Supplies

A diagram of the thrustor electrical system is shown in figure 4, which includes the various power supplies required to start and run the thrustor under pulsed operation at the design point for a typical flight test. Four of these supplies may be considered as "internal" since they supply power at voltages that are relative to the screen of the thrustor. These are the supplies for heating the boiler, energizing the magnetic-field winding, heating the arc-discharge filament, and establishing the discharge potential. All these supplies

were powered through a low-capacitance isolation transformer so that the common screen potential could be rapidly pulsed from 0 to 2450 volts. The other supplies (for neutralizer heating, neutralizer bias, pulsed screen voltage, and pulsed accelerator-grid voltage) were operated relative to the common laboratory (earth-ground) potential. In addition, a thermocouple meter was used for indicating boiler temperature.

Vacuum Facilities

Two vacuum facilities, each with its own internal instrumentation, were used in this project. An 18- by 48-inch chamber was used for initial testing of the thrustor at Space Technology Laboratories. During this time, measurements were also made of the relative concentrations of multiply ionized mercury in the beam. The principle neutralization tests were made in a chamber 84 inches in diameter and 144 inches long. The same thrustor mounting plate together with the insulating Teflon bushing was used to install the thrustor in either chamber.

The thrustor mounting arrangement and the structural details of the 18- by 48-inch chamber are shown in figure 5. Photographic views of the experimental setup are shown in figures 6 and 7. The pumping system for this chamber was a standard commercial assembly incorporating a 7-inch oil-diffusion pump. Tank pressures near the thrustor during operation were of the order of 2×10^{-5} Torr.

The details of the larger chamber are shown in the schematic diagram (fig. 8) and in the interior-view photograph (fig. 9). A liquid-nitrogen-cooled plate was installed near the door to reduce mercury vapor pressure in the vicinity of the thrustor. The chamber was evacuated by an 11-inch oil-diffusion pump. Operating pressures of about 1×10^{-5} Torr were recorded at the downstream end of the tank. The cryobaffle located near the thrustor has a pumping speed for condensable vapors (such as mercury) many times that of the diffusion pump, and the pressures in that region, though not measured, may well have been lower than the measured values.

If the effects of tank pressure on the ion beam are considered, an estimate of the upper-limit values may be made for either a charge-exchange reaction or the ionization of an air molecule. Estimated values of a cross section of the order of 10^{-16} square centimeter and a particle density of about 10^{11} per cubic centimeter (1×10^{-5} Torr) imply a mean free path of about 1 kilometer, or 500 times the length of the beam. Thus, the effects of neutrals should be negligible in the neutralizer tests described herein.

A noteworthy feature of this facility is the instrumentation for diagnosis of the beam that is projected into the tank from the thrustor. For electrical purposes, the far boundary of the tank is the radially segmented collector composed of 6-inch-wide rings 1, 2, 3, 4, 5, and 6 feet in outside diameter. This collector, which is located about 80 inches from the thrustor, is electrically connected to a common point through current-measuring resistors and may be used to gain some information about the ion current density as a function of radius. In front of the collector are two grids that act as a boundary for the fields of electric charges within the tank and that may be biased (as shown in fig. 8) to

prevent either neutralizing or secondary electrons from traversing the space between the first grid and the collector surface. The walls of the tank are lined with three isolated sheet-metal liners each having its own grid. By means of these liners, either electric fields or charged-particle currents directed toward the tank walls can be detected separately. Electric connections from the various rings, plates, and grids within the tank were brought to a patch panel mounted on one of the oscilloscope carts. Here they could be connected in a variety of ways for current or voltage measurements. A typical arrangement is presented in figure 8. The two grids over the collector were tied to the common collector point when the collector was floating.

Each chamber was fitted with a hot-wire emissive probe. In the larger facility, the probe was installed through an available port in the side of the tank at about 70 inches downstream of the accelerator grid. The probe could be moved through its vacuum seal so that the tip (a U-shaped loop, 1/8 in. wide and 3/8 in. long of 0.002-in.-thick tungsten wire) could be placed at any point along a line extending from the axis of the tank to within 5 inches of the tank wall. Measurements of plasma potential could be made with this probe at points along this line by the method described in the section Plasma Potential Measurements.

Neutralizer Configurations

The original neutralizer design of the flight-type thrustor was a V-shaped ribbon of 0.002-inch-thick tantalum located in a plane 1 inch downstream of the accelerator grid with the tip of the V about 3/4 inch from the beam axis and the open end facing radially outward. The location is designated F(3/4, 1), where the numbers in parentheses give the r and z components of the tip position. Extension bars were used to mount the same type of filament in two other fixed positions, namely, F(0, 1) and F(0, 4). Figure 10 shows one of these filaments mounted on a movable arm so that its radial position in the 1-inch downstream plane could be varied through the range -0.5 to 1.5 inches. The movable arm was driven by an insulated shaft that extended through the thrustor mounting plate. This assembly was used in the large chamber. A variable-position neutralizer was also installed as part of the smaller vacuum facility as shown in figures 5 and 7.

Other neutralizer configurations were also tested. One of these was a tantalum ribbon similar to that from which the original neutralizers were formed except that it was left flat and stretched across the beam with its major surfaces parallel to the direction of ion flow. Another neutralizer consisted of two 0.010-inch-diameter tungsten wires stretched across the beam in the 1-inch downstream plane. As a final configuration, a series of shielded wire neutralizers was constructed, as shown diagrammatically in figure 11. The shielded neutralizer with dual 0.010-inch-diameter tungsten wires is shown in figure 12. Altogether, a total of 15 neutralizers (five different types) in several positions were tested during the 27 runs following the initial tests.

PROCEDURE

For assurance that the neutralizer was adequate, it was necessary to

operate the thrustor at or near the "design-point" flight-test conditions. These specifications are given in table I. For vacuum tank tests, the neutralizer was operated at a bias of 20 volts so that electrons were not attracted to the walls during pulsed-beam operation. Although some of the data were obtained at 280 milliamperes thrustor output current, most of the runs were made at a beam current of 200 to 250 milliamperes (70 to 90 percent of rated value). The reduced beam data were obtained at a larger than normal accelerator spacing, which, in turn, reduced the magnitude of the available ion current at low values of accelerator impingement. Also, the open-loop boiler control was unable to provide close temperature regulation; hence, operation was obtained over a range of values of beam current and propellant utilization. However, these operating conditions are near enough to the design point to yield results that will adequately predict neutralizer performance and effectiveness.

The thrustor was placed in operation by heating the boiler after all operating voltages had been applied. When the desired operating conditions were achieved, data were taken by notation of meter readings, by photographing oscilloscope waveforms, and by notation of voltage and current measurements from observation of oscilloscope traces.

Pulsed-Beam Operation

Operation of the ion thrustor in the pulsed-beam mode may be described in terms of the photograph of waveforms shown in figure 13. For convenience, the entire operation was synchronized to the 60-cycle-per-second a-c waveform applied to the thrustor filaments. Special care was taken to make certain that the cathode and neutralizer heating voltages were in phase. A delaying-pulse generator was used to produce a rectangular voltage waveform that could be triggered at any point in the a-c cycle. This waveform was then amplified by two high-voltage pulse amplifiers, one connected to the screen and the other to the accelerator grid of the thrustor that supply, respectively, the 2500- and -2000-volt acceleration potentials. The duty cycle of the acceleration-voltage pulses was variable through almost the entire range from 0 to 1. Generally, a duty cycle of about 0.95 was used with the off pulse set to occur just before the end of the neutralizer heating interval.

Heating current to the neutralizer filament was supplied through a silicon rectifier, so that heating occurred only during one-half of each power-line cycle. During the other one-half of each cycle, the neutralizer remained hot and emissive but did not experience a longitudinal voltage gradient due to heating current and was therefore a unipotential source of electrons.

Plasma-Potential Measurement

The approximate value of plasma potential was given by the floating-collector potential. The pair of traces in figure 13(f) show the floating-collector potential for two values of neutralizer heating voltage and demonstrate how this measurement was used. During the lower of these two traces the neutralizer was hot enough to provide adequate emission throughout the cycle, and the floating-collector potential closely corresponds to the average potential

of the neutralizer. The upper trace was taken with a lower neutralizer temperature and barely adequate emission. During the middle portion of the waveform, the neutralizer had cooled off with the result that it was beginning to run emission-limited. The resulting slight deficiency in neutralizing current was sufficient to cause a 10-volt increment in plasma potential in this instance. A further slight decrease in neutralizer temperature at this point would have resulted in much more drastic changes in plasma potential. Continuous monitoring of the floating-collector potential was used to ensure that the neutralizer was running space-charge-limited, while more precise measurements were being made.

A few measurements were made of plasma potential by observing the floating potential of an emissive probe (fig. 14(a)). But the most precise measurements were made by observing the cutoff characteristic of the emissive probe. The probe was heated by rectified a-c current in the same manner (and same phase) as the neutralizer, as shown in figure 14(b). Its temperature was adjusted so that it could emit a current of about 1 milliampere, which is a low value compared with the total beam current. The probe potential was accurately adjusted by using a differential voltmeter accurate to ±0.005 volt. The potential drop across the current-measuring resistor, due to the difference between emitted current and current collected from the plasma (at some point on the time axis, e.g., 3 msec from the start of the acceleration voltage pulse) was observed on an oscilloscope with a sensitive d-c preamplifier. The probe was then cooled sufficiently so that its electron emission was cut off, and the consequent shift in resistor voltage drop was noted. The probe potential was then shifted to a new value, the shift in resistor voltage drop was noted for the same shift in filament temperature at this new potential, and so on. The resulting values of electron emission for a range of probe potentials were then plotted on semilog graph paper, and intersection of the emission-limited characteristic with the cutoff slope was taken as the plasma potential. It is believed that this use of the hot-wire probe is novel, and a brief theoretical discussion is included herein for clarity.

When immersed in the plasma beam, the emissive probe forms the cathode of a thermionic diode and the plasma is the anode. The emission of such a cathode may be described separately in three regions:

(1) With a high positive applied potential, the saturation current is governed by the Richardson equation:

$$I_s = K_1 T^2 e^{-\epsilon W/kT}$$

where K_1 is a geometric constant, T is Kelvin temperature, ϵ is the electronic charge, W is work function potential, and k is the Boltzmann constant.

(2) In the region of retarding potentials applied to the diode, the emission is governed by the Maxwell-Boltzmann temperature distribution of the thermionic electrons according to the relation:

$$I = I_o e^{-\epsilon\varphi/kT}$$

where I_o is the zero potential current and φ is the magnitude of the

retarding potential.

(3) In the intermediate region, the space-charge-limited current is governed by Child's law.

At a filament temperature where the emissive probe is at the plasma potential that will generate only a very small space-charge cloud, the transition region in the cutoff characteristic is small. In a semilog plot of emitted current against diode voltage at a fixed filament temperature, a fairly sharp break occurs at the zero potential point.

From reference to the circuit in figure 14(b), three currents may be identified that contribute to the voltage drop across the measuring resistor. The first is the ion current that is collected by the probe. This current has a value independent of probe potential for the range of interest and is negligibly small because of the minute projected area of the probe filament. The second is the current of electrons (Langmuir probe current) that the probe collects from the beam. This current is frequently measured even with the "hot" probes. Above the plasma potential, the semilog plot of this current departs from a straight line whose slope is related to the "Maxwellian temperature" of the electrons in the plasma. However, if the electron energy distribution is not Maxwellian, no straight-line portion exists; and, frequently, the point of departure is not as precisely indicated as desired. In any case, the Langmuir probe current is independent of filament temperature at any particular value of probe potential. The third current is the electron current that is emitted into the plasma beam and may be used, as indicated previously, for the precise measurement of plasma potential. It should be noted that the slope of the emission cutoff characteristic is related to the "temperature" of the emitted electrons or of the probe filament. As shown later, such things as noise in the beam, modifications of the local plasma potential by the probe, and secondary emission of electrons may change the apparent slope of this cutoff. These effects are most noticeable in the low-current part of the characteristic away from the indicated intersection.

In practice, the emitted-electron-current magnitude may be separately observed by alternating the filament temperature at each value of probe potential. Between the chosen "hot" (emission-limited) value and some lower temperature, at which the electron emission is cut off, the filament is hot enough to maintain a "clean" (constant work function) surface.

Other Measurements

Measurements of beam current density were made by photographing oscilloscope traces of the waveforms of current to the several collector rings. For this purpose, each ring was biased at 15 to 20 volts, in turn, so that the ion current could be seen. The photographs were then measured, and the values of current and current density at chosen points on the time axis were plotted.

The time-of-flight of ions in the beam was measured by observing the delay from the beginning of the acceleration voltage pulse to the onset of collector current. Measurements of ion velocity were made with a crossed-field velocity filter (figs. 15 and 16). Incidental measurements of the relative abundances of multiply ionized atoms were made this way.

From the notations of heater voltage and current readings at the neutralizer power supply, it was possible to compute the conductance of the neutralizer filament as a function of its lifetime.

RESULTS AND DISCUSSION

Data are given herein for 11 of the 15 neutralizers tested, including four V-shaped flight-type and one or more of each of the other types. The lifetime data include the experience of more than one test for several of the filaments, whose history is given.

Ion-Velocity Measurements

Two methods were used for measurement of ion velocity: One method was the direct observation of ion transit time from the thrustor to the downstream collector, and the other involved the use of a crossed-field velocity filter. Figure 17 shows the result of the time-of-flight measurement. The transit time of a singly charged mercury ion in the larger chamber was 41 microseconds, while that of the doubly charged ion was only 0.707 as long. Accordingly, the onset of the principal collector current at 41 microseconds following the start of the accelerating voltage pulse was preceded by a smaller current step at about 29 microseconds. These values are in agreement with the calculated singly charged ion velocity of 4.85×10^4 meters per second which corresponds to a net acceleration potential of 2450 volts. These transit times and their magnitudes give evidence that substantial neutralization of the beam is being achieved.

A schematic drawing of the ion-velocity filter is shown in figure 15 and the device itself is shown in figure 16. Ions that are directed into the sampling tube (fig. 5) enter the drift tube through the entrance slit. There they encounter opposing forces perpendicular to their drift velocity because of the presence of a constant vertical magnetic field and an adjustable horizontal electric field. For a given particle species, the net deflecting force can be adjusted to zero. Such particles enter the exit slit and produce a signal at the target. The driven-shield cathode follower is sensitive to currents of millimicroamperes and has a rise time at this current level of about 1 microsecond. Accordingly, the signal from the velocity filter preserves the time-of-flight information and is indicative of that current of particles which passes through undeflected.

From both the time-of-flight and velocity-filter measurements, it was noted that about 6 percent by number (12 percent by current) of the ions were doubly charged. This result is in good agreement with values reported in reference 7, for the same (50 v) discharge potential. As the discharge potential was in-

creased to over 100 volts, the presence of triply ionized mercury could be observed in the time-of-flight observation.

Emissive-Probe Data

All the emissive-probe data were taken during that portion of the cycle when both the emissive probe and the neutralizer were unipotential electron sources. Under these conditions, the confusing effects of voltage gradients along the neutralizer and the probe filaments were eliminated. Also, the plasma beam collector was connected to the thrustor through a high impedance (1 megohm), that is, essentially floating.

Some examples of emissive probe characteristics that were obtained during this project are shown in figure 18. The curve in figure 18(a) exhibits a sharp break and leads to a measurement of plasma potential ($\delta V = V_{cutoff} - V_{neutralizer}$) with an accuracy of the order of 0.1 volt. In figure 18(b), the ends of the characteristic are straight but the knee of the curve is rounded off. The curve of 18(c) shows a general rounding, while in 18(d) precise values in the cutoff region were difficult to obtain because of noise, as indicated by the extension of the upper and lower boundaries of the data points. Deviations of these curves from the sharp break are not completely understood; however, certain features have been related to known conditions. For example, a slope in the emission-limited region of the curve is likely to occur as a result of sputtering erosion of the emissive-probe filament. The approximate time required to obtain data to plot one of these curves is 10 to 20 minutes. Slow changes in filament emission over this time show up as a slope. Rounding of the break in the curve may be due to rapid fluctuations in the local plasma potential as the result of noise in the beam or to local perturbation of the plasma potential by the minute electron current that the probe emits.

The first phase of the program included work on the V-shaped tantalum filament neutralizer, the ribbon neutralizer, the wire neutralizers, and one shielded neutralizer. During this time, two general classes of emissive-probe measurements were made. In the first, measurements of potential were made as the probe was changed in radial position for each of several data points. In the second series, the position of the probe was fixed and the potential of the beam measured as the position of the neutralizer relative to the beam was varied. The results of the first series of measurements are shown in figure 19; those of the second series are shown in figure 20.

During the second phase of the work, three other versions of the shielded neutralizer were examined. The emphasis during this phase was on filament lifetime, and only a few emissive-probe measurements were made to determine a single value of the plasma potential in each case. These tests were performed in the smaller of the two vacuum facilities, and the probe was necessarily much closer to the thrustor than it had been in the larger chamber (10 in. from thrustor). As a final check on the comparison between probe measurements at the two axial positions, one measurement was made of plasma potential with a V-shaped tantalum filament centered in the beam. This gave a value of δV equal to 7.3 volts near the thrustor that could be compared with the lowest point on the

curve of figure 20. Allowing a tolerance of 0.5 volt on these measurements, there is evidence of a 3- to 5-volt potential gradient in about a 6-foot length of plasma beam.

The cutoff characteristic of an emissive probe has been the means for making plasma-potential measurements of such precision that a quantitative comparison of several neutralizer configurations is possible. For example, the coupling between the original flight-type filament and the plasma is increased somewhat if the filament is moved into the center of the beam, but it is considerably decreased when the neutralizer is moved downstream. The closest coupling was obtained with the immersed wires, and the flat ribbon of the centrally located V-shaped filament displayed similar behavior. Interposing a shield between the wires and the beam extended the life of the wires, as is discussed in the section Neutralizer Lifetime, at only a slight cost in coupling, although attempts to seclude the wire deeply within the shield gave rise to plasma potentials many times those of the highest values obtained during the first phase of the tests. In general, the emissive-probe measurements have confirmed the adequacy of the flight-type neutralizer system and have pointed out some directions along which further development may proceed.

Floating Emissive Probe

If the emissive probe is returned to "ground" through a high-impedance load resistor (fig. 14(a)), it will assume a potential at which an equality exists between the emitted and collected currents and the current through the load resistor. Since the ion current is small because of the minute projected area of the probe filament and since the load resistor current is also small, the floating-collector potential is very nearly that at which the emitted current to the beam is equal to the Langmuir probe electron current, which the probe collects. In this configuration, the probe may be used for continuous observation of the plasma potential. However, the indicated potential is a function of probe filament temperature, plasma density, and load resistance; and, consequently, its accuracy is limited to about a volt. Floating-probe and floating-collector waveforms are presented in figure 21 for three cases of coupling between the beam and neutralizer. In figure 21(a) the original fixed-position (F(0.75,1)) neutralizer only was used. Figure 21(b) was recorded when the variable-position neutralizer was in use and was located at the axis (F(0,1)). Figure 21(c) was obtained when both neutralizers were used simultaneously.

The floating-probe waveforms observed were similar in appearance to the floating-collector waveforms but were generally higher than the collector potentials sometimes by as much as a few volts. This difference is ascribed primarily to the presence of a plasma sheath over the collector surface.

The plasma-potential measurements made by a floating-collector, a floating-emissive probe, or an emissive probe cutoff characteristic have led to the following conclusion: The precise measurement of the probe cutoff characteristic is required to measure differences among a group of effective neutralizers, whereas the momentary operating condition of any one neutralizer (i.e.,

whether it is operating space-charge-limited and hence is doing the best it can) may be more readily ascertained by using the more approximate measurements. In the actual spacecraft application of an ion thrustor, the use of a floating collector will not be possible, and it may well be that the floating emissive probe will be a useful instrument for continuously monitoring beam neutralization.

Neutralizer Lifetime

The results of the neutralizer conductance and lifetime measurements are shown in figure 22 for the neutralizers referred to in figure 19. Maximum lifetimes of from 2 to 3 hours were typical of the immersed ribbon and wire filaments. The rate of change of conductance was considerably more gradual for the shielded wires. An extrapolation of this slope out to a 50-percent loss of conductance (approximate typical failure point) would predict a lifetime of about 25 hours for the first shielded configuration.

A physical examination of the first shielded neutralizer revealed that, of the two wires, the one farther downstream had suffered most of the sputtering erosion. In subsequent runs, a series of shielded neutralizers were used, each having a single wire at some specified distance from the shielding bar. Measurements were made of plasma potential and rate of change of conductance. These results are summarized in the following table:

Neutralizer	Spacing from shield, mm	δV (near thrustor), v	Conductance loss rate, percent/hr
13	2 to 3	12	1.0
14 -	4	8 to 15	4.0
15	1.5 to 2	55 to 58	.2

The data for conductance loss rate are plotted in the expanded scale of figure 23. From these results, it is evident that some compromise exists between filament seclusion and electrical coupling to the plasma.

Beam Current Density

Figure 24 shows examples of the plots of ion currents and of ion current densities as functions of beam radius at the collector position (about 80 in. downstream of the thrustor). At the left is a plot of current to each ring in milliamperes, while at the right there is a normalized plot of current density. The two cases are for (a) a floating collector, in which case the neutralizing current must equal the ion current, and (b) a collector at ground potential (about 20 v more negative than the neutralizer). In this case, the plasma potential subsides below that of the neutralizer and cuts off the current from the neutralizer after the first ion transit time. It is noteworthy that there is no

marked difference between the two plots, as might have been expected if additional dispersive effects were present due to lack of space-charge neutralization.

The fraction of the total ion momentum that is directed along the beam axis was computed for the two cases presented from the equation

$$\langle \cos \theta \rangle = \frac{\int i \cos \theta \, d\theta}{\int i \, d\theta} \simeq \frac{\sum i_k \cos \theta_k}{i_{total}}$$

where i_k is the current to a given collector ring, and θ_k is the mean angle between the beam axis and the trajectories to the ring. This value is about 0.98 for both cases.

CONCLUDING REMARKS

It is understood that the operation of ion thrustors in spacecraft is not likely to include pulsed acceleration voltages or the heating of filaments by pulsating direct current. However, it was the object of this study to observe coupling of the neutralizer to the plasma beam and the relation of this coupling to geometric configuration under conditions that would minimize the effects of nongeometric factors. The techniques described herein were intended for this purpose. A tradeoff is possible between neutralizer coupling and sputtering erosion for the immersed type of neutralizer configuration. What may be a satisfactory compromise between the two is represented by the shielded neutralizer configuration. The experiments reported herein are only exploratory and do not represent the optimum in shielded design.

With regard to the neutralizer coupling measurements, it should be noted that the plasma potentials reported from the first phase of these tests were the values obtained under a particular set of conditions, namely, with the emissive probe about 70 inches from the thrustor and the plasma incident upon a floating collector a few inches farther away. Unfortunately, it was not possible to make axial scans of the plasma potential in the large tank. Such measurements on lower voltage cesium beams in smaller tanks have indicated that negative-potential gradients exist along the axis in these beams. If measurements are made far enough downstream, a potential equal to or slightly lower than that of the neutralizer may be reached. In view of this, the plasma-potential measurements reported here for the electron-bombardment thrustor are offered as indications of the comparative coupling among a number of geometric configurations. These measurements should not necessarily be interpreted as indicating the maximum of electron injection potential that may occur in a region near the neutralizer.

Finally, the degree of coupling observed was in all cases sufficient to affect both current and space-charge neutralization of the ion beam to the extent that no measurable additional electrostatic divergence of the beam was found over and above the amount due to accelerator optics. This, of course, was true under the condition that the neutralizer filament was sufficiently heated to

operate in a space-charge-limited mode. Assurance that this condition was realized in a flight test could be given either by testing the actual flight-test thrustor by using a floating collector (or isolated thrustor) before launch, or by using some beam diagnostic device such as a floating emissive probe in the flight-test package to measure the plasma potential. It may be concluded that the original design of the neutralizer should be satisfactory both in coupling and lifetime for short duration flight tests, but improvements in lifetime will be necessary for eventual use in spacecraft propulsion. Means of improving both the coupling and the lifetime have been pointed out in this study.

REFERENCES

1. Sellen, J. M., Jr., and Kemp, R. F.: Cesium Ion Beam Neutralization in Vehicular Simulation. Preprint 61-84-1778, Am. Rocket Soc., Inc., 1961.

2. Kemp, Robert F., Sellen, J. M., Jr., and Pawlik, Eugene V.: Beam Neutralization Test of a Flight Model Electron Bombardment Engine. Paper 2663-62, Am. Rocket Soc., Inc., 1962.

3. Kaufman, Harold R.: An Ion Rocket with an Electron-Bombardment Ion Source. NASA TN D-585, 1961.

4. Reader, Paul D.: Investigation of a 10-Centimeter-Diameter Electron-Bombardment Ion Rocket. NASA TN D-1163, 1962.

5. Kerslake, William R.: Accelerator Grid Tests on an Electron-Bombardment Ion Rocket. NASA TN D-1168, 1962.

6. Pawlik, Eugene V., and Wenger, Norman C.: Performance Evaluation of a Mercury-Propellant Feed System for a Flight-Model Ion Engine. NASA TN D-1213, 1962.

7. Milder, Nelson L.: Comparative Measurements of Singly and Doubly Ionized Mercury Produced by Electron-Bombardment Ion Engine. NASA TN D-1219, 1962.

TABLE I. - THRUSTOR OPERATING SPECIFICATIONS FOR TYPICAL FLIGHT TEST

Component	Voltage, v	Current, amp	Nominal operating power, w	Operating point
Boiler	0 to 40 a.c.	0 to 4	as required (~10)	370° to 400° F
Magnetic field	6 to 10 d.c.	18	180	30 gauss
Cathode	9 to 10 a.c.	20 to 25	220	Cathode temperature set to give 5-amp discharge
Discharge	50 d.c.	5	250	
Neutralizer heater	9 to 10 a.c.	20	200	$I_{neut} = I_{beam}$
Positive acceleration (screen) potential	2500 d.c.	$I = I_{beam}$ 0.280	725	2500 v
Negative acceleration (accel grid) potential	-2000 d.c.	0.004 to 0.010	----------	-2000 v
Neutralizer bias	20 for these laboratory tests 0 for flight tests	----------	----------	----------

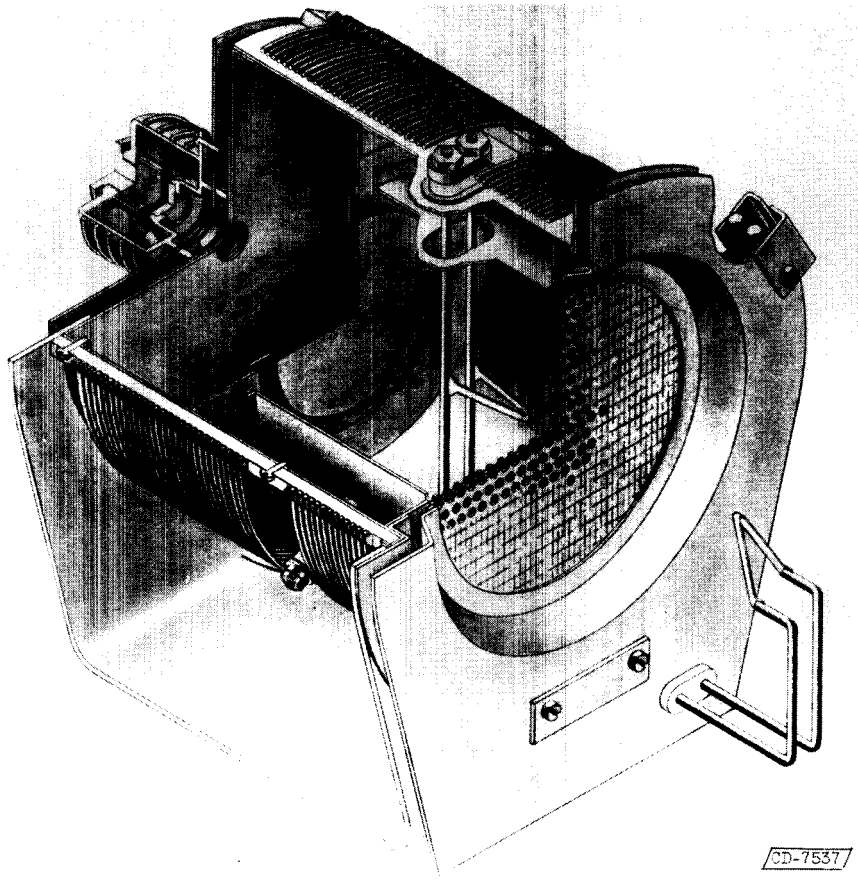

Figure 1. - Flight-model electron-bombardment thrustor.

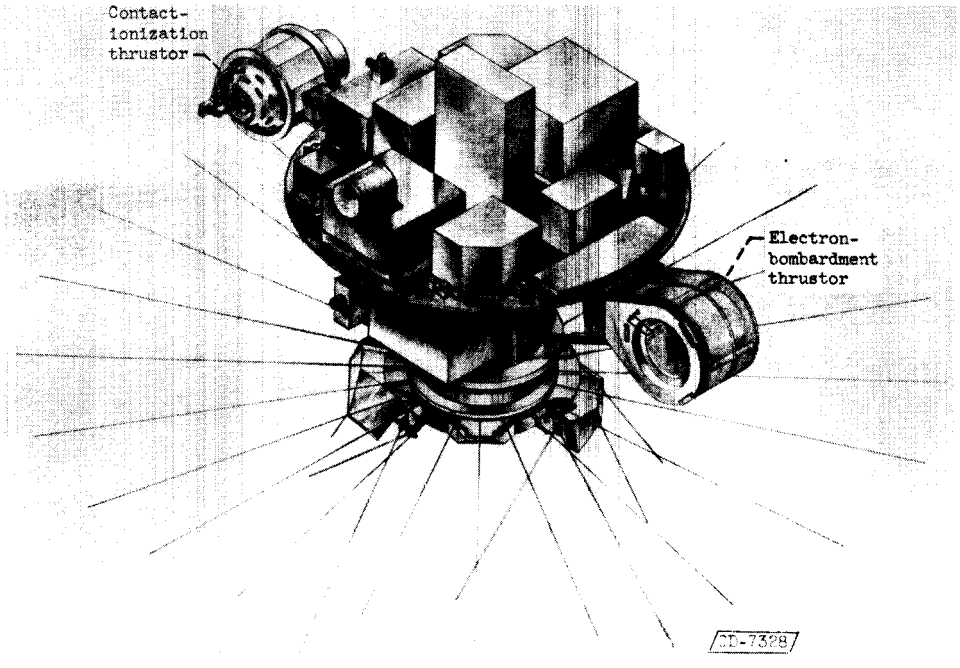

Figure 2. - Proposed flight-test package.

C-63926

Figure 3. - Flight-model thrustor mounted for ground-facility testing.

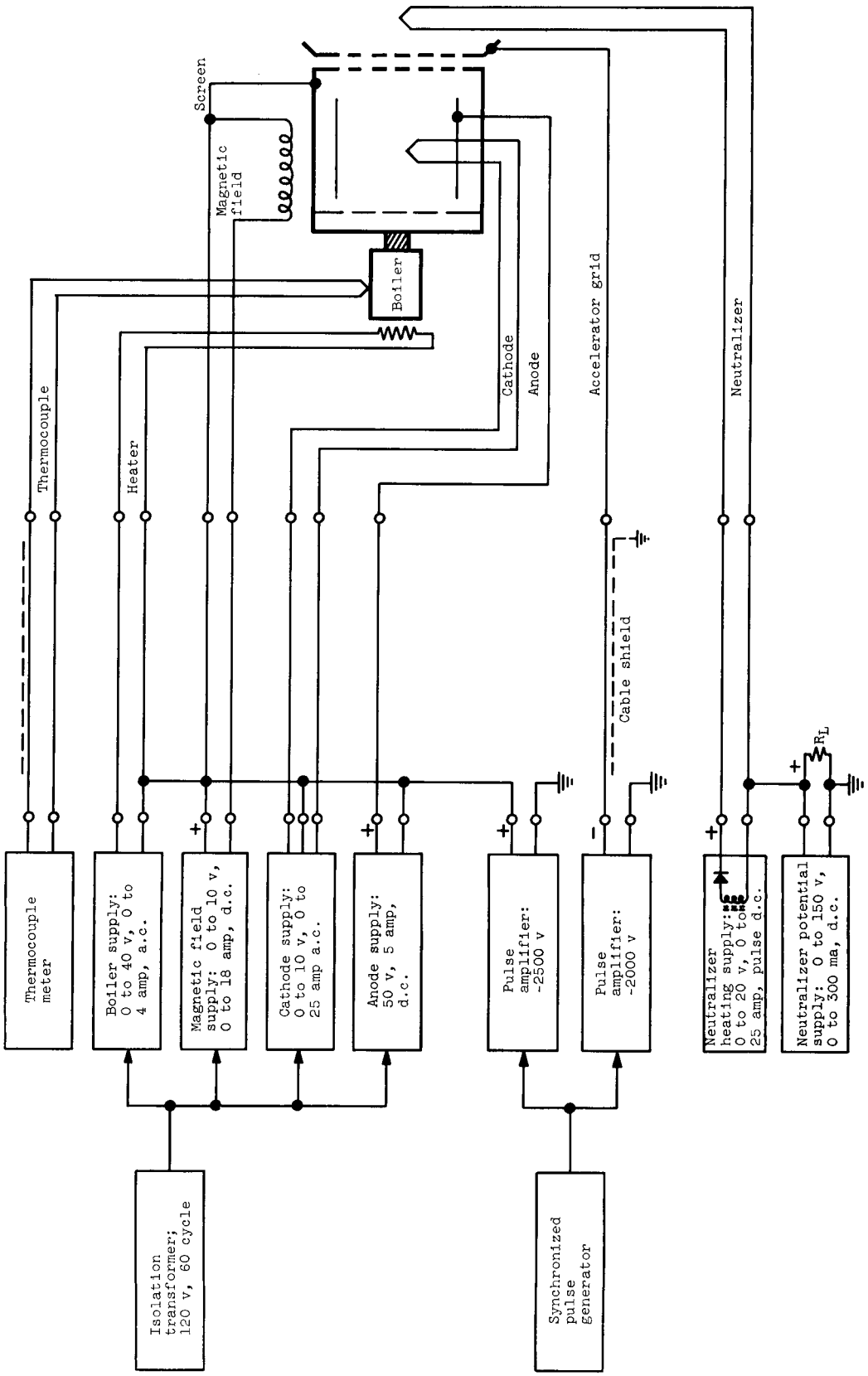

Figure 4. - Diagram of thrustor electrical system.

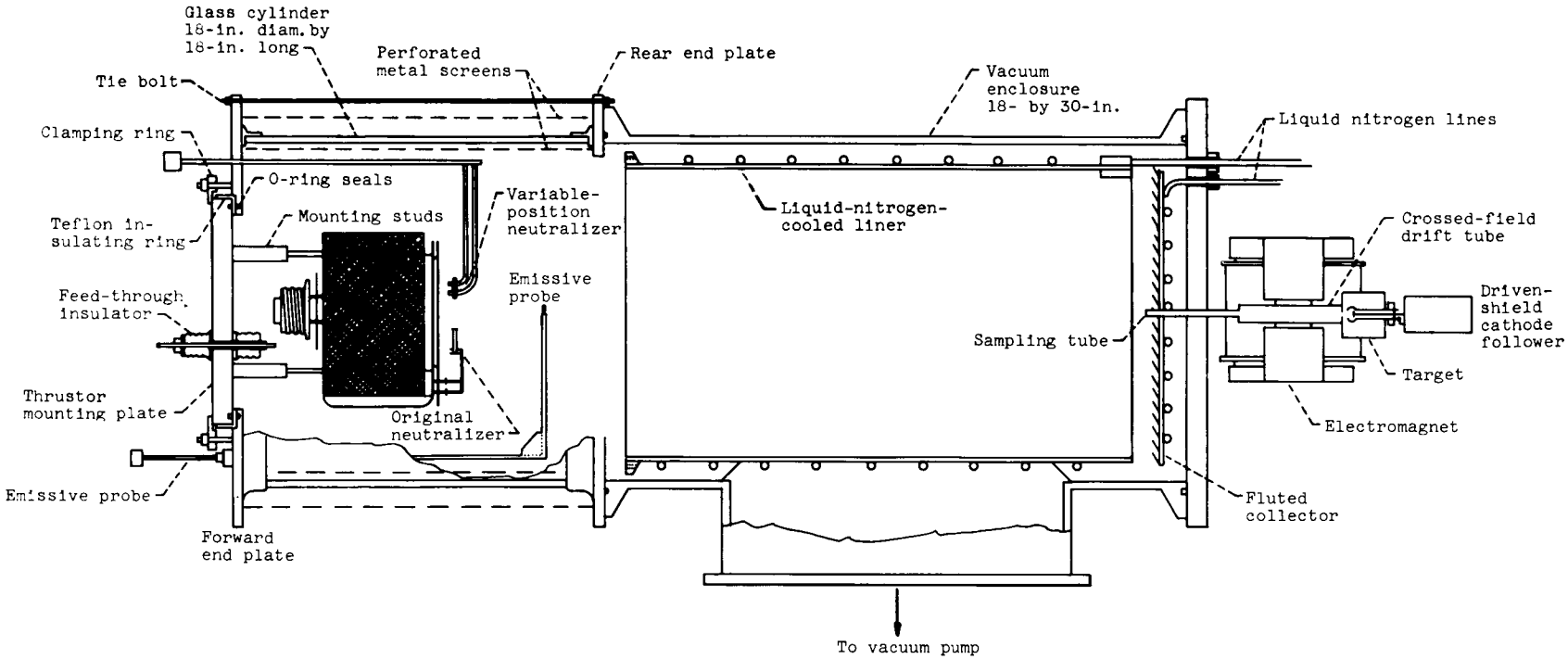

Figure 5. - Structural details of the 18- by 48-inch vacuum facility showing thrustor mounting arrangement.

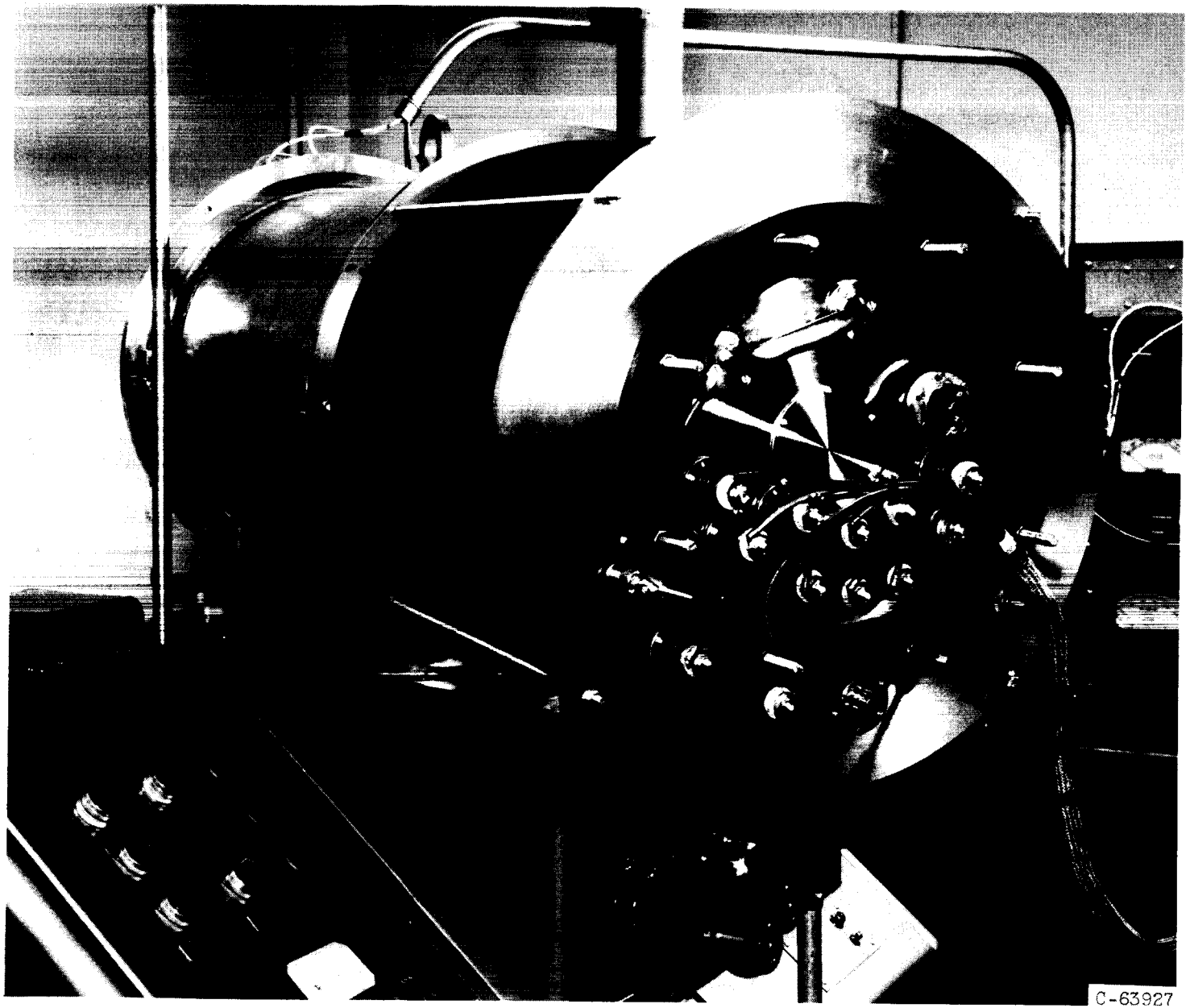

Figure 6. - Electrical connections to thrustor mounting plate.

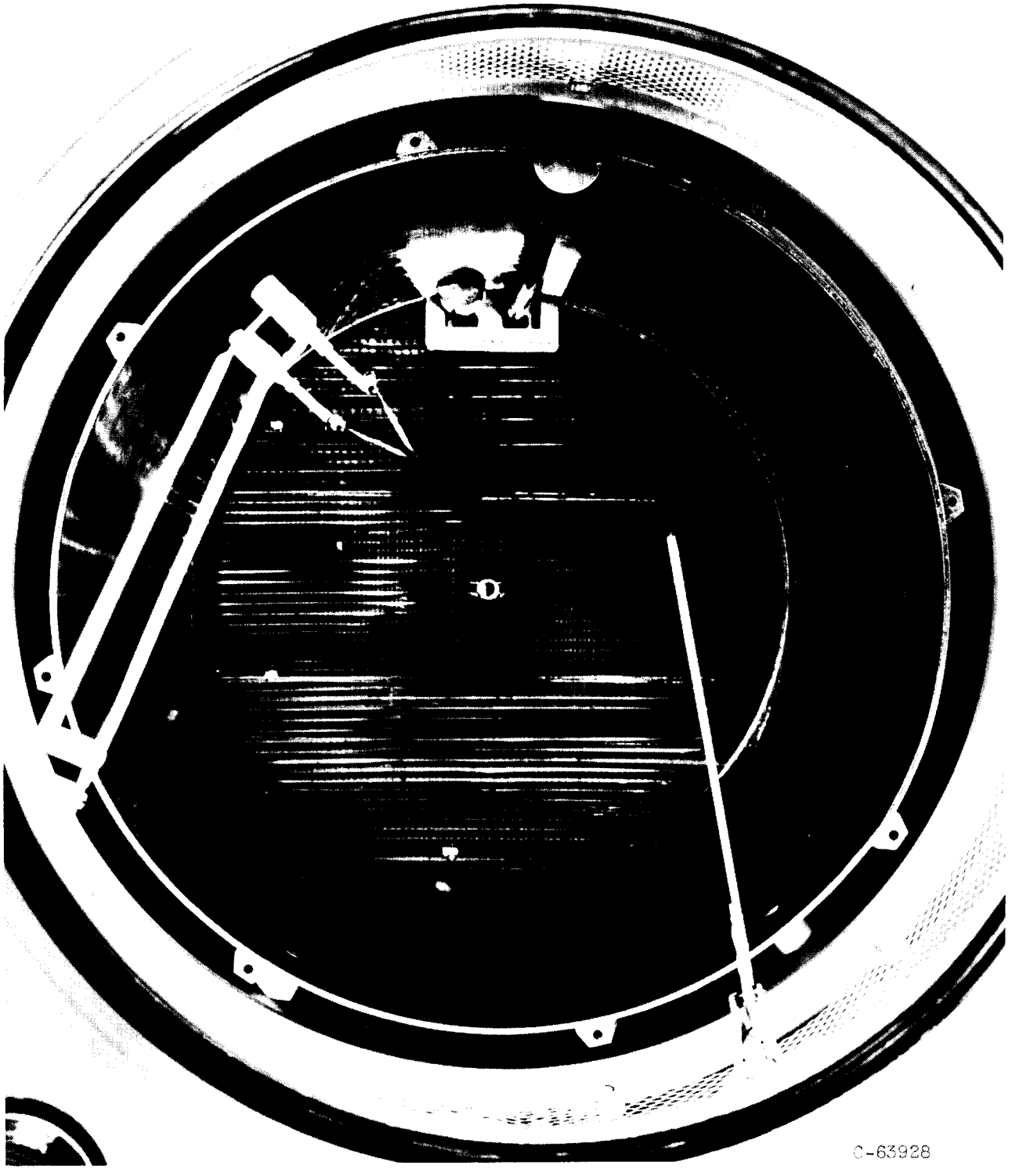

Figure 7. - Interior view of the 18- by 48-inch vacuum tank showing variable-position neutralizer, emissive probe, cryogenic wall liner, and beam collector.

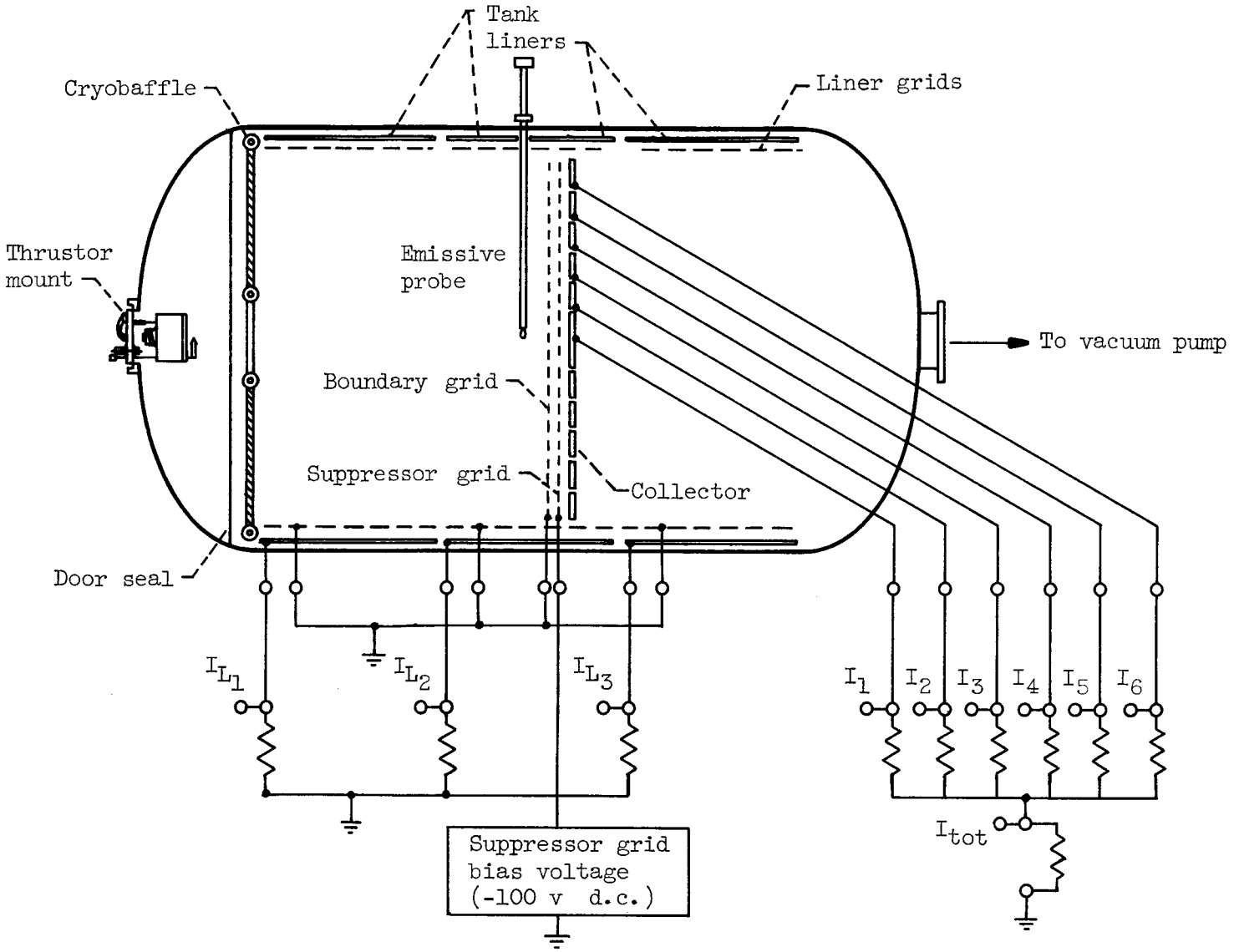

Figure 8. - Schematic diagram of 84- by 144-inch vacuum chamber. All resistors are 10 ohms.

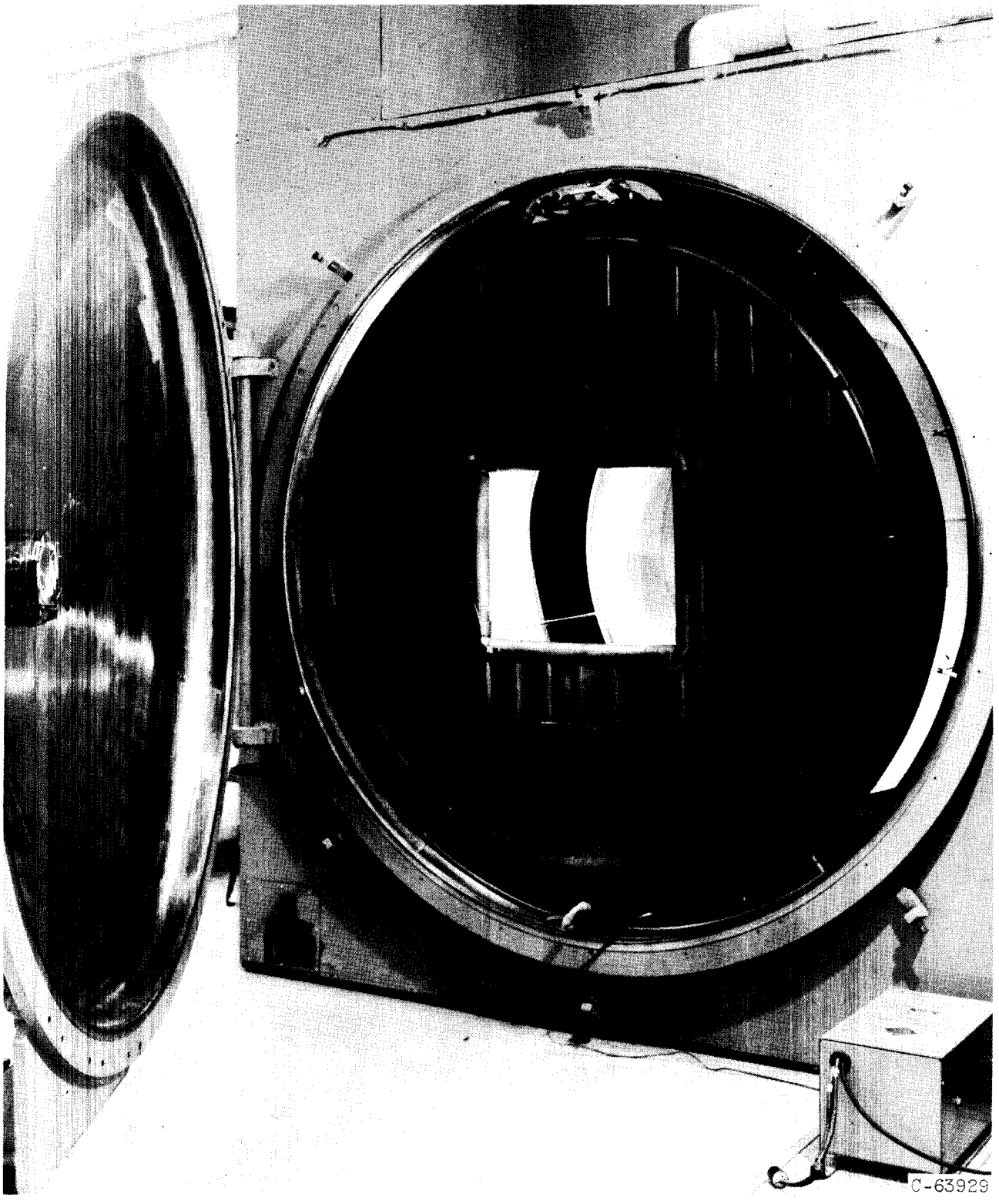

Figure 9. - Interior view of 84- by 144-inch vacuum chamber showing thrustor mounting and cryobaffle. A portion of collector, liners, and grids are visible through baffle opening.

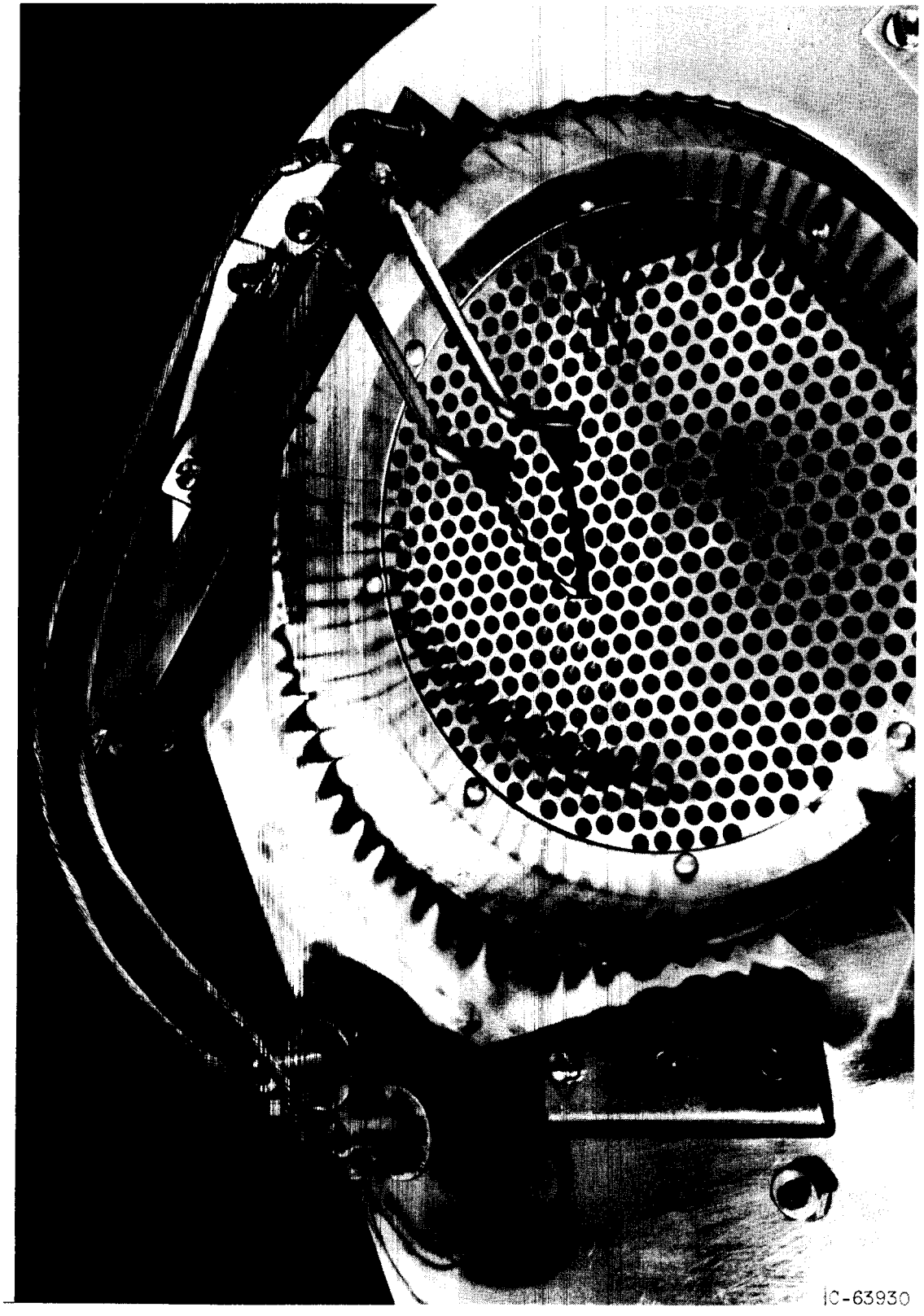

Figure 10. - Variable-position neutralizer with V-shaped tantalum ribbon.

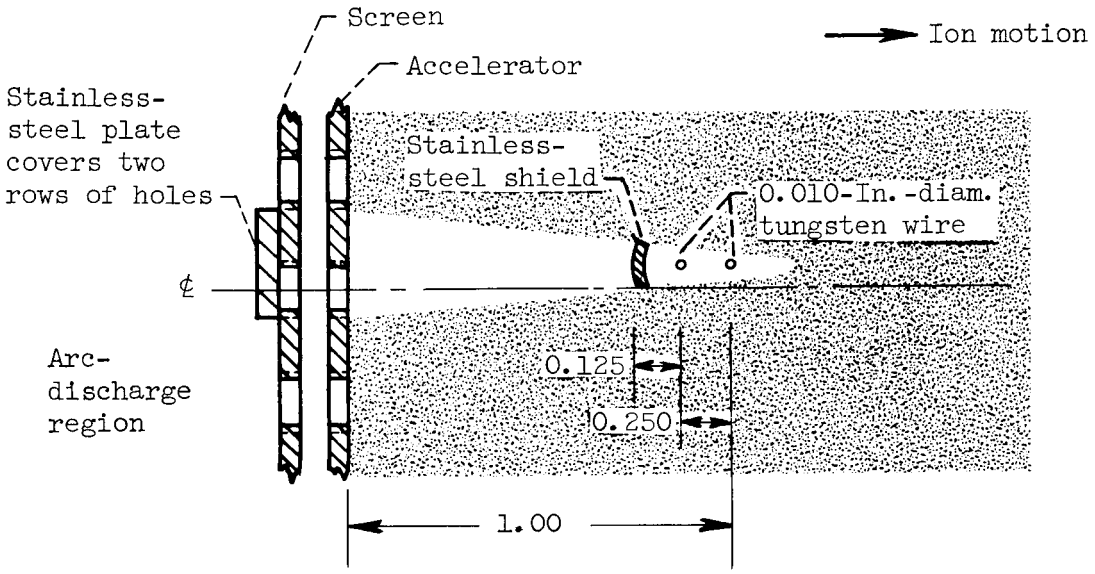

(a) Double wire shielded neutralizer.

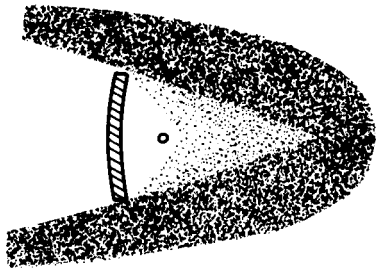

(b) Suggested detail in ion shadow to account for the gradual improvement in wire lifetime as it is moved closer to shield.

Figure 11. - Cross-sectional view of shielded neutralizer.

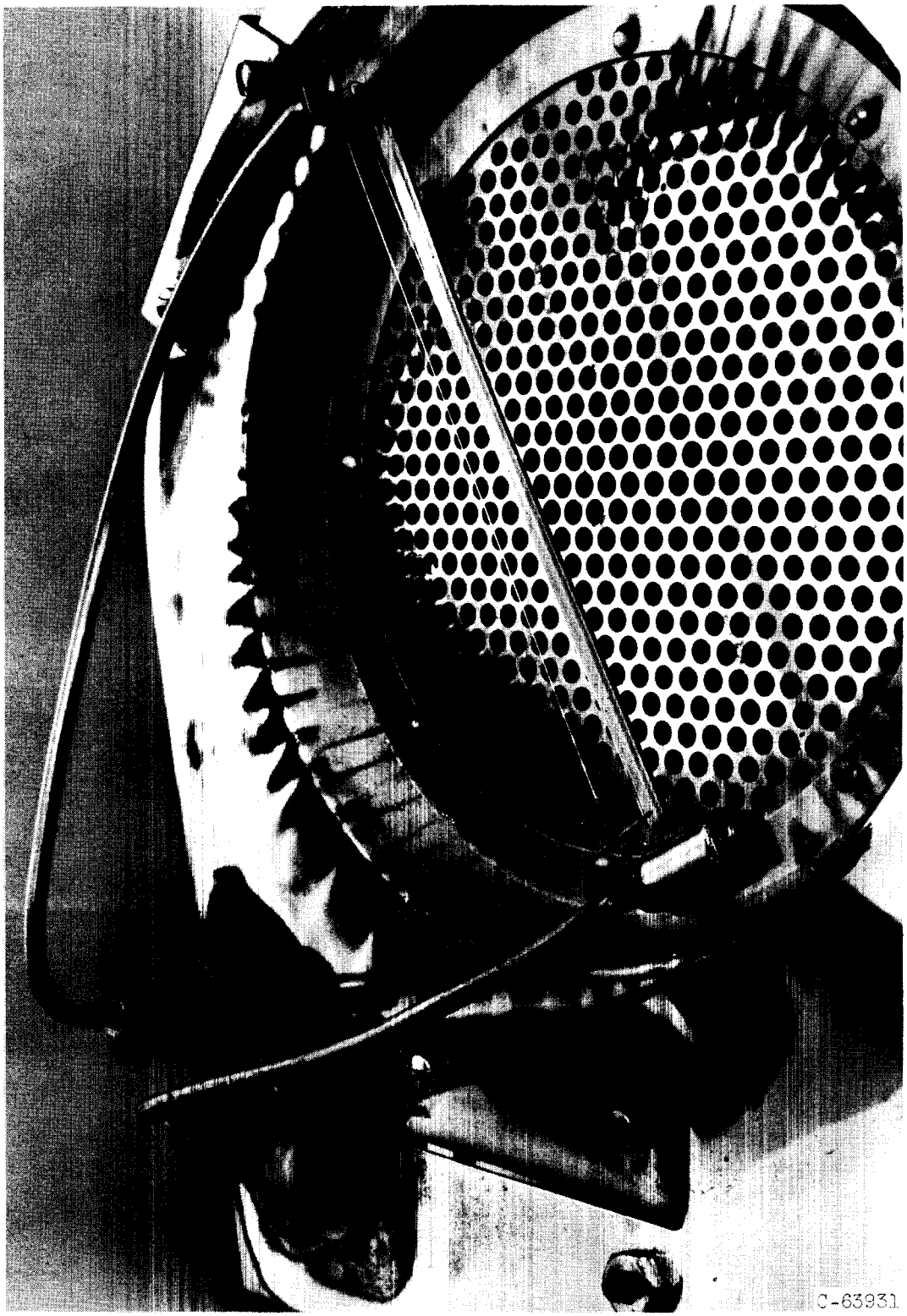

Figure 12. - Shielded neutralizer with dual 0.010-inch-diameter tungsten wires.

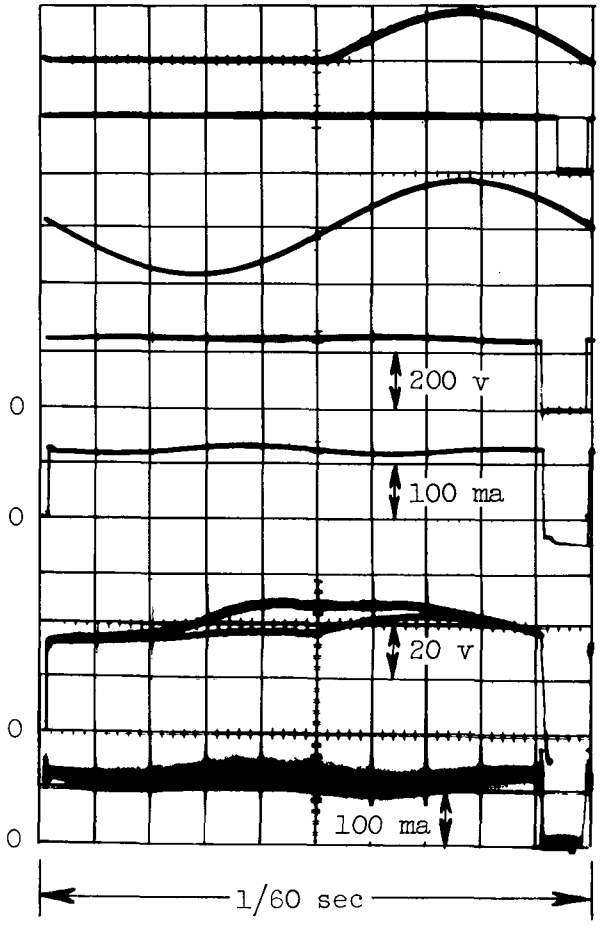

(a) Heater voltage across neutralizer.

(b) Pulser input signal.

(c) Cathode heating.

(d) +2.5-kv pulser.

(e) Collector current (collector grounded).

(f) Floating-collector potential.

(g) Floating-collector neutralizer current.

Figure 13. - Characteristics and synchronization of significant waveforms.

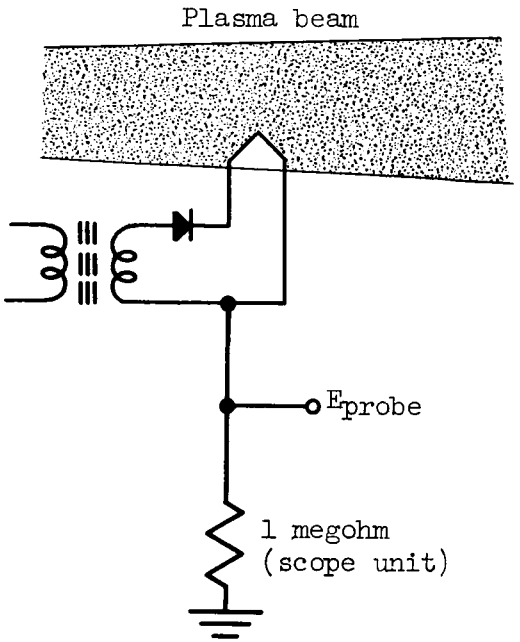

(a) Floating probe circuit.

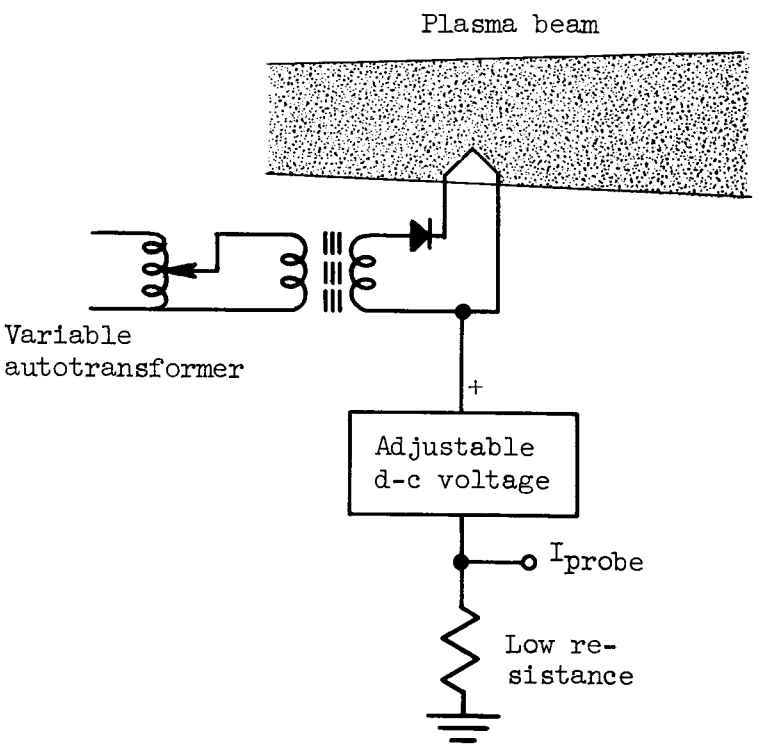

(b) Circuit for measuring emission cutoff characteristics.

Figure 14. - Emissive probe.

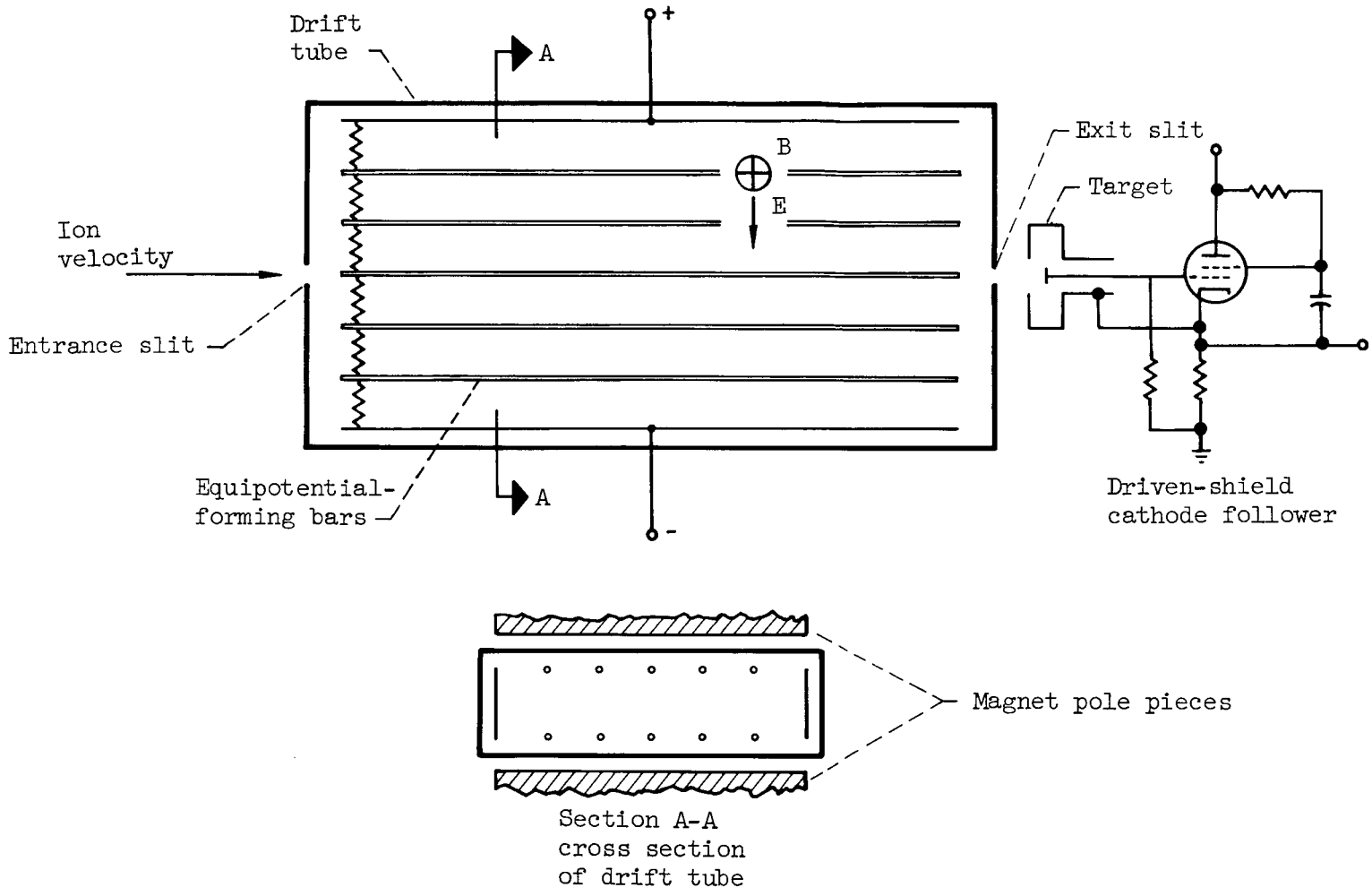

Figure 15. - Schematic diagram of the crossed-field ion-velocity filter.

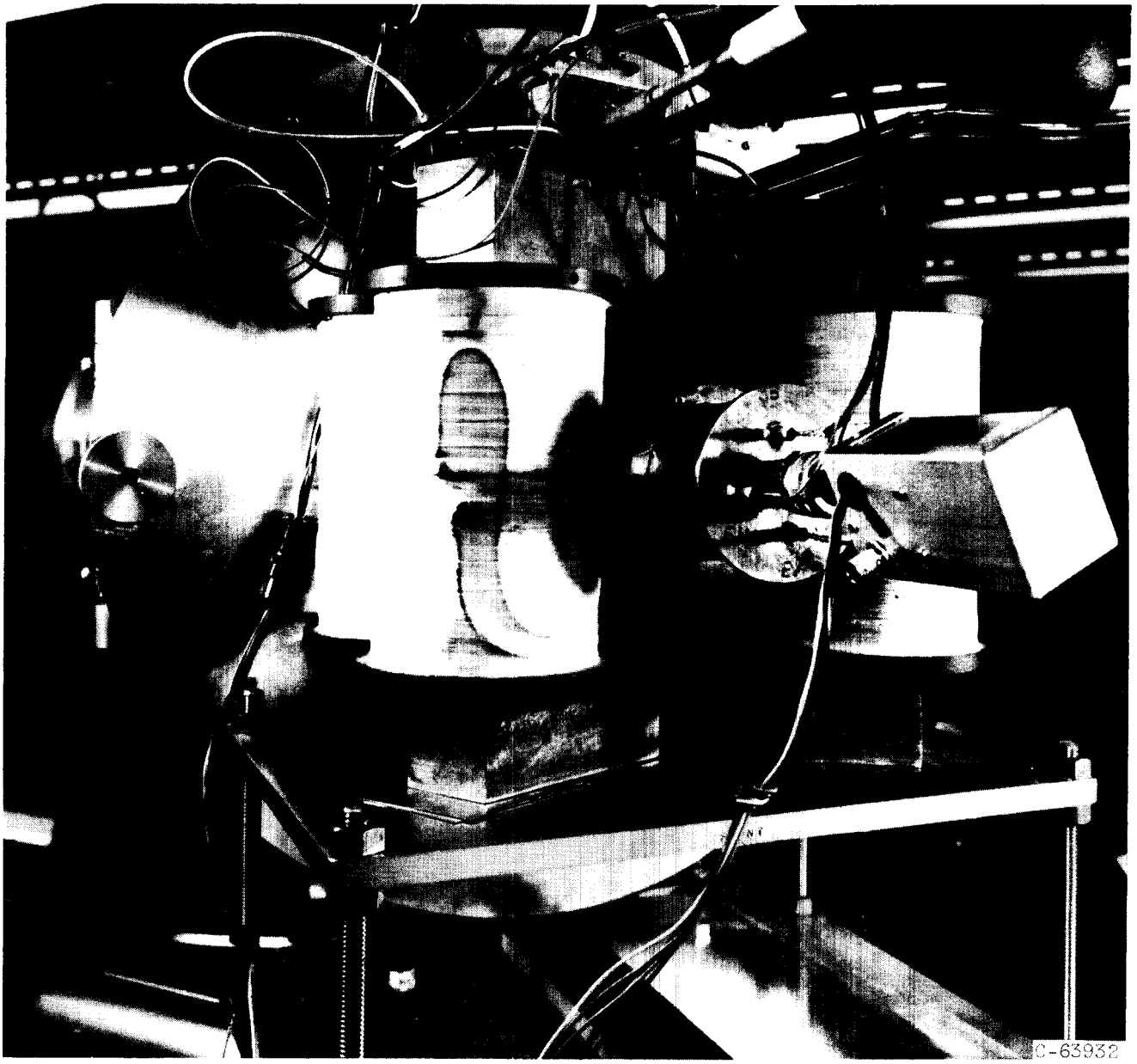

Figure 16. - Rear view of the 18- by 48-inch tank showing electromagnet, target chamber, and amplifier of crossed-field velocity filter.

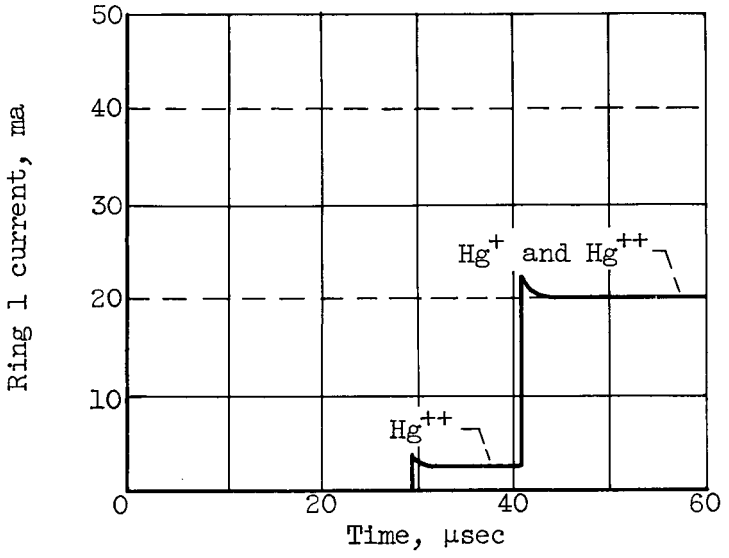

Figure 17. - Current signal to collector ring 1 for first several microseconds following start of acceleration voltage pulse. This waveform is a measure of the transit time and relative concentrations of singly and doubly ionized mercury atoms.

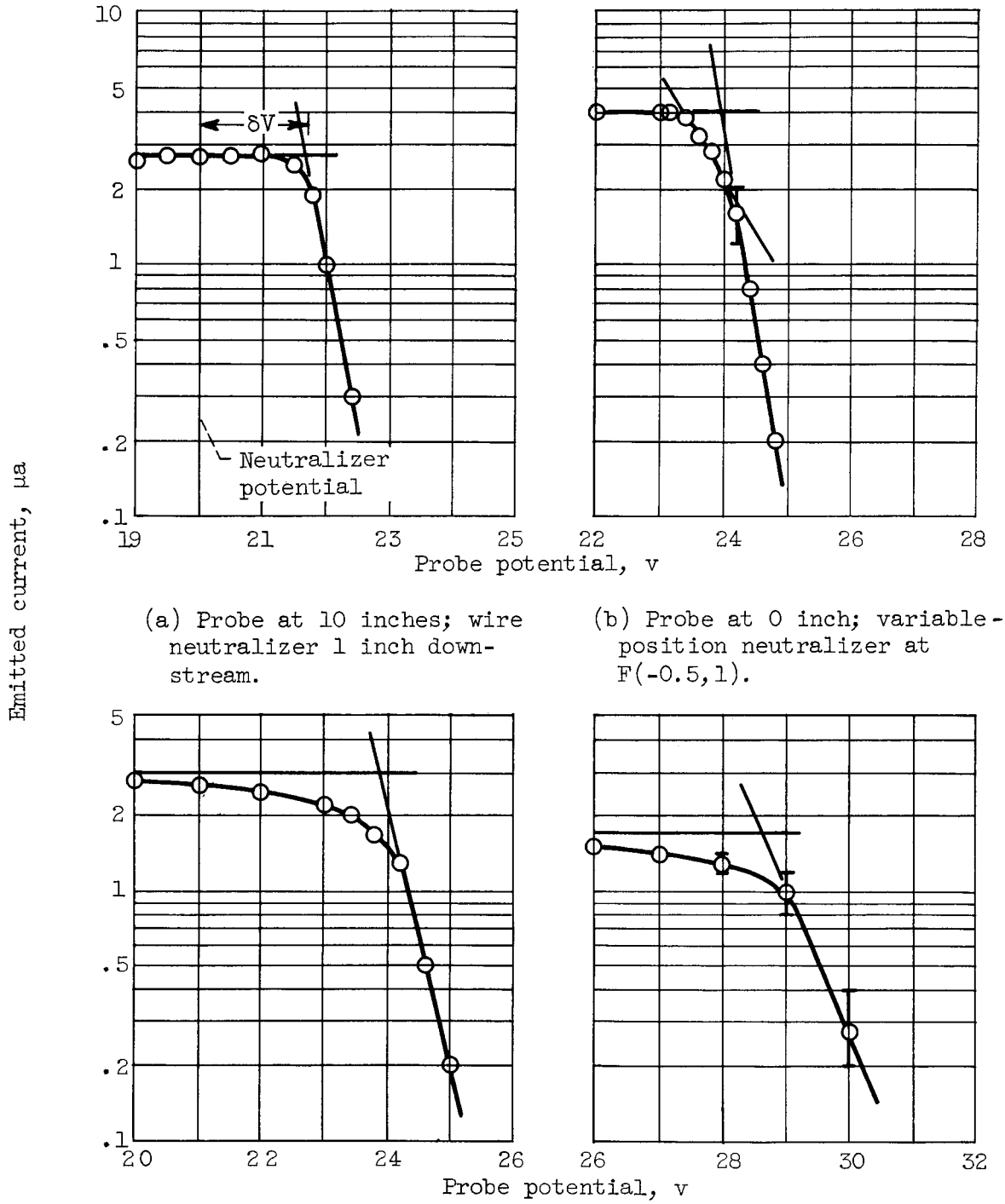

(a) Probe at 10 inches; wire neutralizer 1 inch downstream.

(b) Probe at 0 inch; variable-position neutralizer at F(-0.5,1).

(c) Probe at 0 inch; variable-position neutralizer at F(0,1).

(d) Probe at 0 inch; original neutralizer at F(0.75,1).

Figure 18. - Examples of emissive-probe characteristics that were obtained during the neutralization tests. Radial position of probe is indicated. Neutralizer potential, 20 volts.

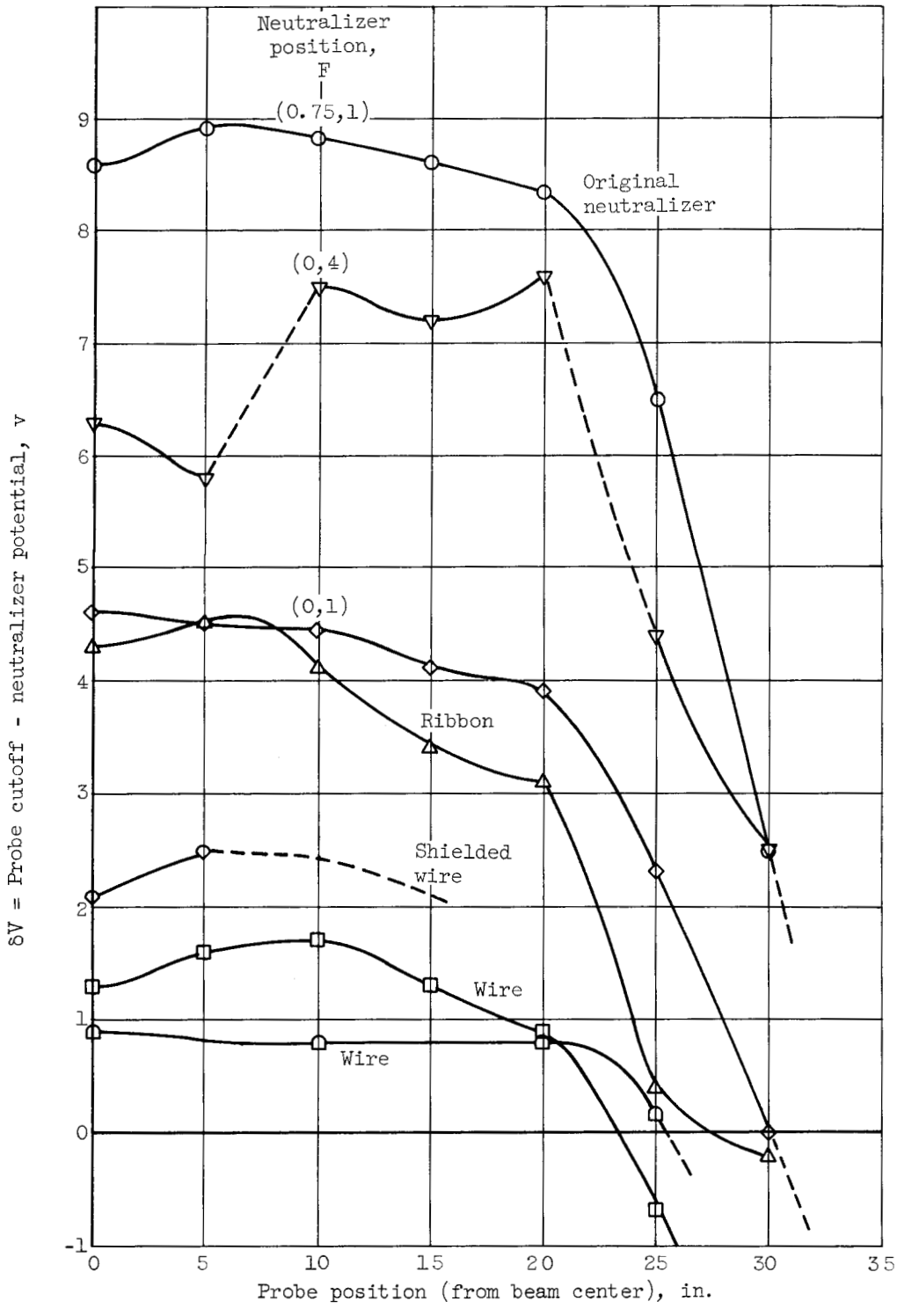

Figure 19. - Emissive-probe measurements of plasma potential relative to that of the neutralizer as a function of the neutralizer position and configuration. The probe is on the axis of the beam, 70 inches downstream. The wire and ribbon neutralizers were located about 1 inch downstream of the accelerator grid.

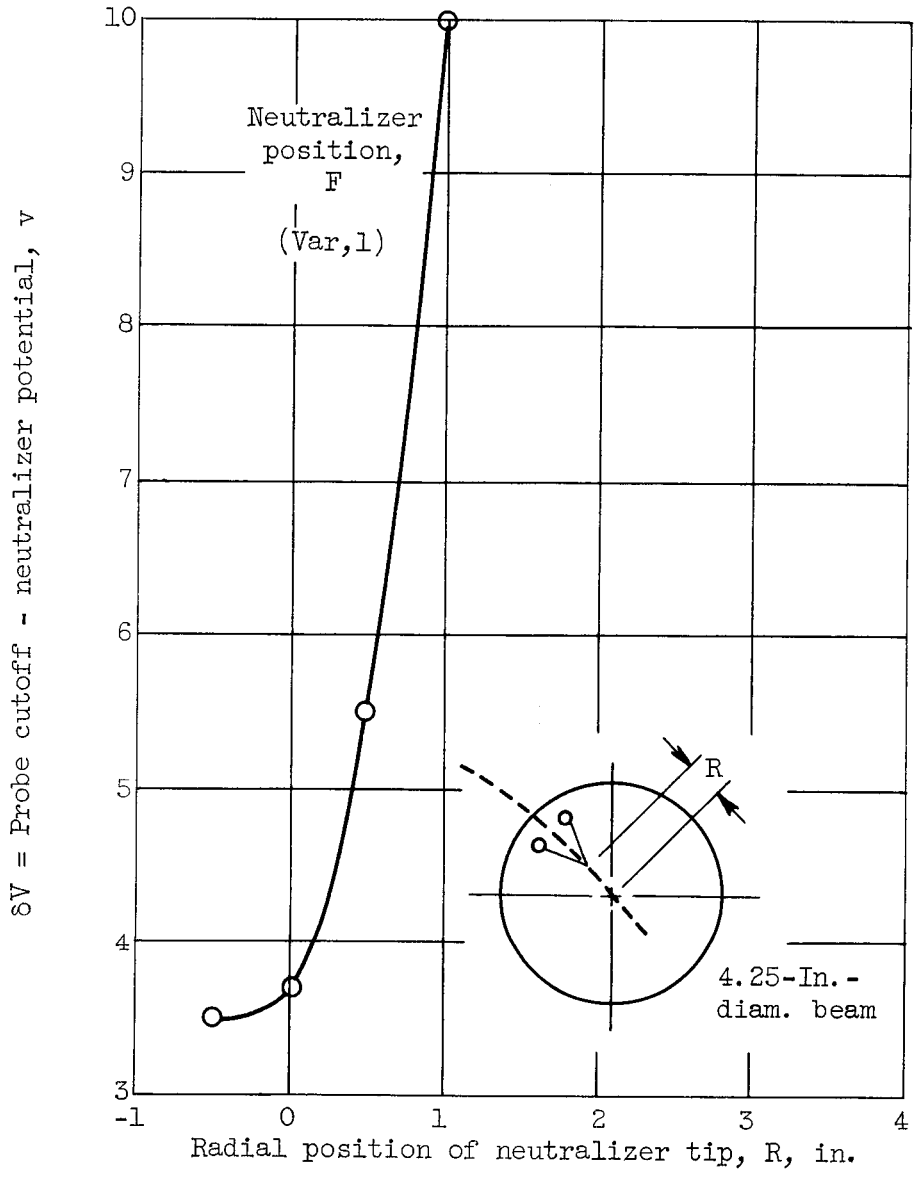

Figure 20. - Emissive-probe measurements of plasma potential relative to that of neutralizer as a function of position of variable-position neutralizer. Probe is on axis of beam, 70 inches downstream of accelerating grid.

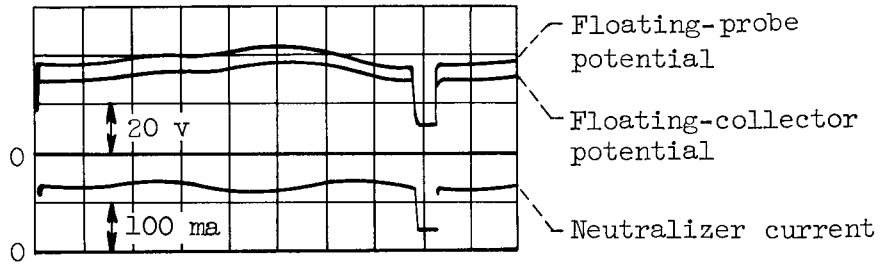

(a) Fixed-position neutralizer.

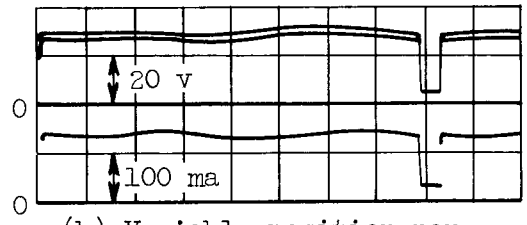

(b) Variable-position neutralizer centered in beam.

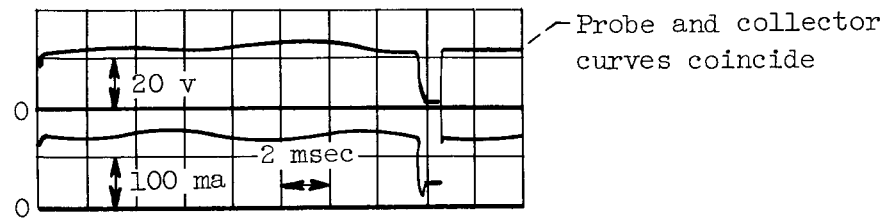

(c) Fixed-position plus variable-position neutralizer centered in beam.

Figure 21. - Floating-emissive-probe and floating-collector waveforms. Neutralizer potential, 20 volts.

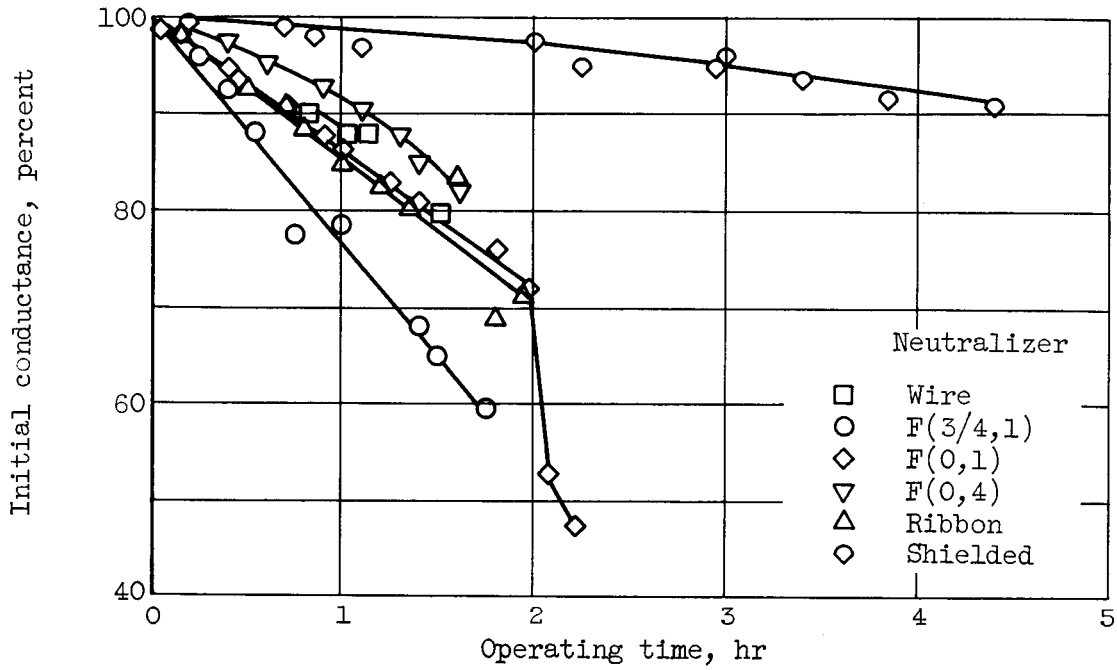

Figure 22. - Neutralizer filament conductance measurements.

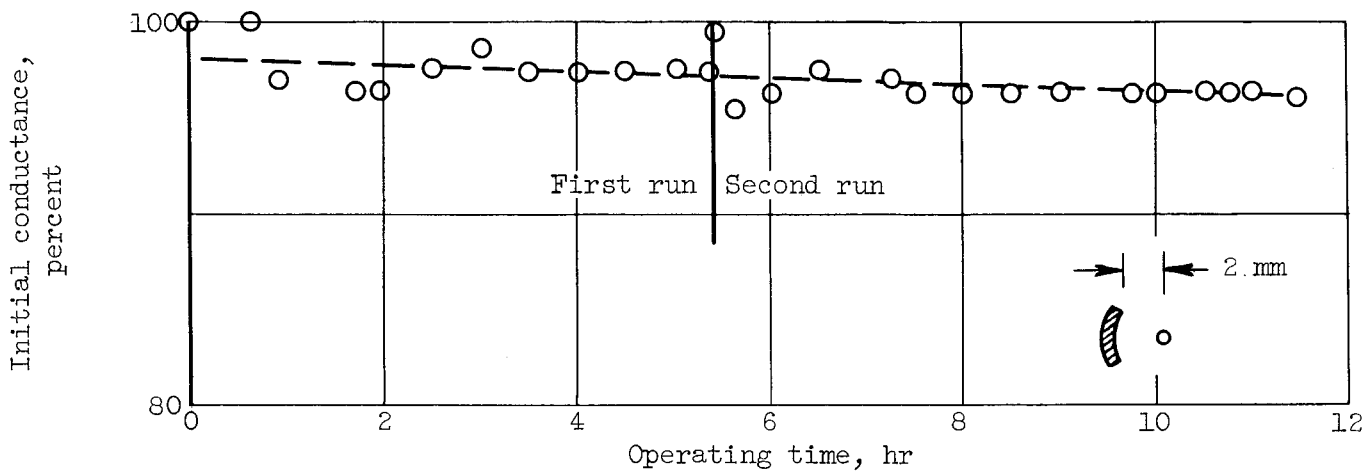

Figure 23. - Conductance measurements for a well-shielded neutralizer wire.

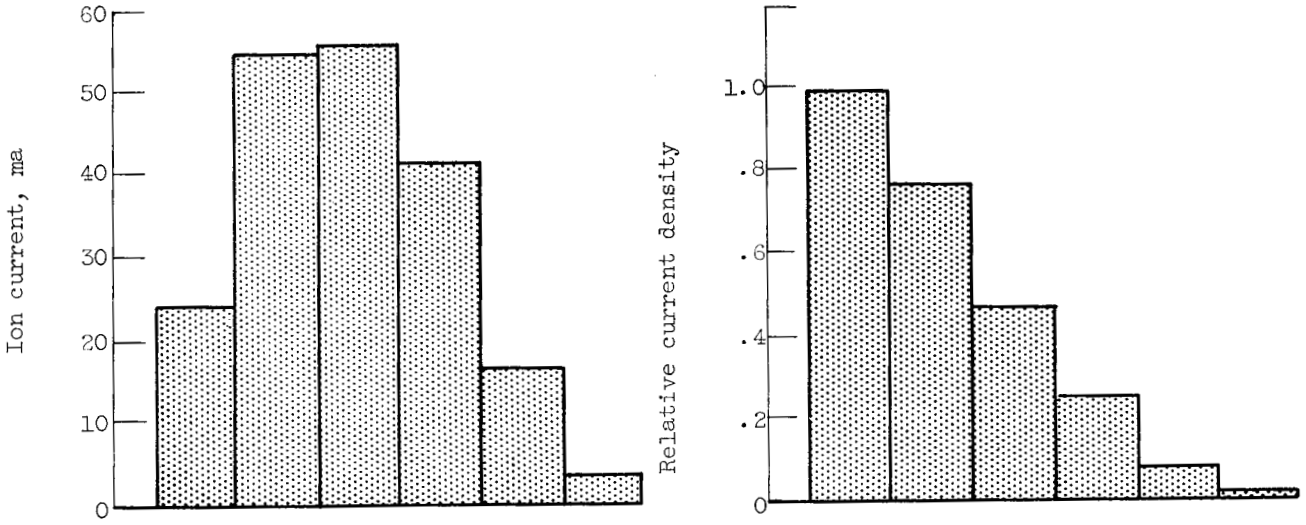

(a) Floating collector. Total current, 197 milliamperes; $\langle \cos \theta \rangle = 0.981 = \cos(11.1^{\circ})$.

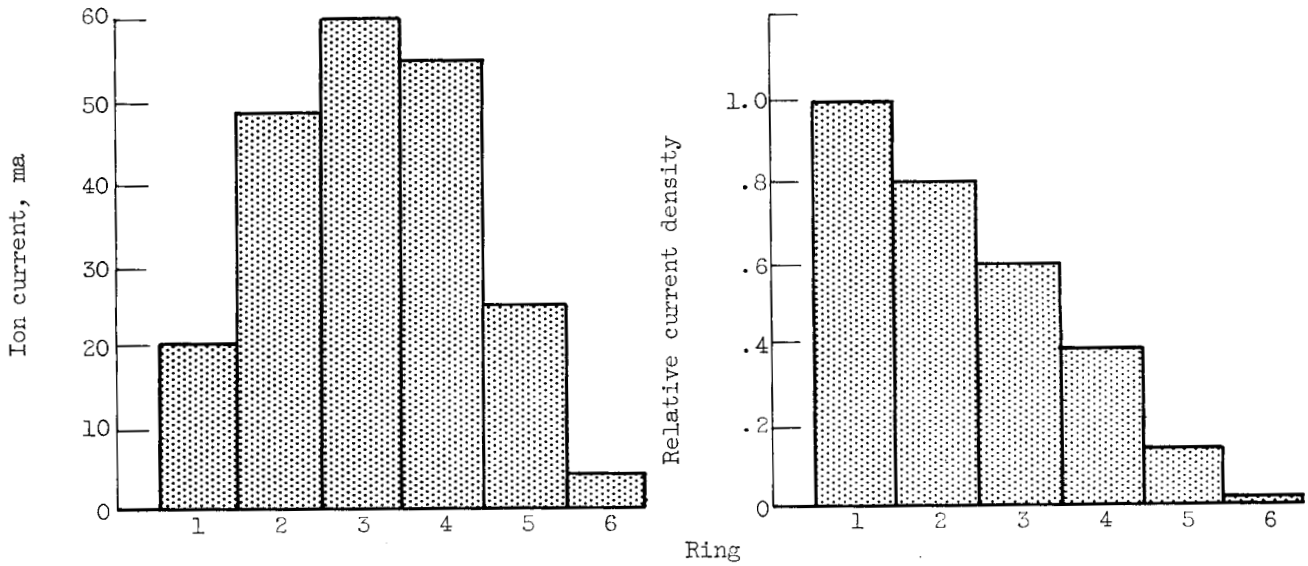

(b) Grounded collector. Total current, 213 milliamperes; $\langle \cos \theta \rangle = 0.977 = \cos(12.1^{\circ})$.

Figure 24. - Ion currents and ion current densities at the collector position. The diameters of the rings in the collector are 1, 2, 3, 4, 5, and 6 feet. The collector is about 80 inches downstream of the thrustor position.